Effect of Acute Experimental Pulmonary Arterial Occlusion on the Deposition and Clearance of Technetium-99m-DTPA Radioaerosols

Yutaka Mori,* Philip O. Alderson and Howard L. Berman

Department of Radiology, Columbia-Presbyterian Medical Center, New York, New York

Canine models of autologous PE and balloon occlusion of the pulmonary vasculature were used to evaluate radioaerosol deposition and to quantify radioaerosol clearance in the immediate postembolic period. **Methods:** A total of 28 animals were anesthetized, intubated and studied (central balloon occlusion = 4, peripheral balloon occlusion = 7, autologous PE = 5, various control groups = 12). A gamma camera computer system was used to monitor the distribution and clearance rate of inhaled DTPA radioaerosol. The perfusion defect distribution was determined after the radioaerosol study using ^{99m}Tc-MAA. **Results:** A new radioaerosol deposition defect was seen in 3 of 16 animals in a zone of acute vascular occlusion by a balloon (n = 2) or PE (n = 1). In addition, radioaerosol clearance rates were altered substantially. Peripheral vascular occlusion and PE caused radioaerosol clearance rates to accelerate significantly (control clearance half-time = 33.6 ± 4.6 min, post-balloon occlusion = 19.0 ± 8.3 min, post-PE = 12.4 ± 3.7 min, both p < 0.05). In only one case did these clearance rate changes create a visible abnormality in the aerosol images. **Conclusions:** The pulmonary deposition patterns and clearance rates of ^{99m}Tc-DTPA radioaerosol can be altered by acute vascular occlusion or PE. These findings should be considered when interpreting radioaerosol images in patients with suspected PE.

Key Words: pulmonary embolism; radioaerosols; animal models; technetium-99m-DTPA

J Nucl Med 1994; 35:1351–1357

Radioaerosols of ^{99m}Tc-DTPA are often used to provide the "ventilation" adjunct to perfusion lung scintigraphy in patients suspected of having pulmonary embolism (PE). Particulate radioaerosols, however, are affected more significantly by air flow abnormalities in large airways than are radioactive gases, and large airways are known to undergo constriction in response to acute PE (*1*). Accordingly, radioaerosol deposition patterns might be more perturbed than those of radioactive gases by the acute effects of PE on pulmonary ventilation. Bronchoconstriction could lead to accumulation of radioaerosol activity proximal to the embolized zone or even in the perihilar region secondary to larger, more central PE.

Bronchoconstriction also could lead to regional deposition defects similar to those induced infrequently by PE in the distribution of ^{133}Xe gas in the immediate postembolic period (*2,3*). Acceleration of ^{99m}Tc-DTPA radioaerosol clearance across the alveolar-capillary membrane also has been reported as a consequence of PE (*4*). The changes in clearance rate induced by PE are said to be confined to the zones distal to emboli, and to be a possible source of misinterpretation of aerosol-perfusion studies for PE. Despite these observations and theoretical considerations, little has been written about the ways in which PE affects radioaerosol deposition and clearance. In the current study we have employed a combination of previously described animal models to pursue these objectives.

MATERIALS AND METHODS

Animal Models

Twenty-eight mongrel dogs weighing 20–25 kg each were studied. Each dog was anesthetized by intravenous administration of 30 mg/kg of sodium phenobarbital and then intubated. Additional doses of sodium phenobarbital were administered during the course of the experiment to maintain adequate levels of sedation. Each animal was connected to a Harvard respirator cycled at a ventilation volume of 300–350 cc and a respiratory rate of 15 breaths per minute with periodic hyperinflation.

Each animal had a baseline ^{99m}Tc-DTPA radioaerosol study as described below. Forty-eight hours later, each animal was reanesthetized and intubated for a study involving one of three vascular occlusion models: main pulmonary artery balloon occlusion (n = 4); pulmonary arterial balloon occlusion at a more peripheral (fourth-order) vascular level (n = 7); or autologous pulmonary thromboembolism (n = 5). Because of the baseline

radioaerosol study, each animal served as its own control. Twelve other animals were used for additional control experiments as described below.

Unilateral pulmonary artery balloon occlusion was performed as follows. Both common femoral veins were percutaneously catheterized utilizing standard Seldinger technique. Vascular sheaths (8-Fr) were positioned in each vessel. Under fluoroscopic guidance, a 7-Fr cobra catheter (Cook, Inc., Bloomington, IN) was atraumatically advanced over a floppy guide wire through the right side of the heart into the main pulmonary artery. The catheter was then advanced into either the right or left main pulmonary artery. Renografin 76% (10 cc) was then slowly hand-injected to confirm appropriate catheter position. After confirming satisfactory position, the balloon was inflated to occlude the artery.

Peripheral balloon occlusion was performed in similar fashion with the following exceptions. Using a 0.038-inch heavy duty exchange guidewire, the cobra catheter was replaced with a 7-Fr Berenstein 13-mm occlusion balloon catheter. Under fluoroscopic guidance, the catheter was advanced distally to the fourth order (i.e., segmental) level. Renographin-76 was again used to confirm appropriate catheter position and the balloon was inflated to occlude the vessel. Just before moving the animal to the adjacent gamma camera room, a chest radiograph was taken to visualize the catheter and to exclude opacities and volume loss in the catheterized region.

Autologous thromboemboli were created in an isolated jugular vein segment while each animal lay supine. A vein segment approximately 2 inches in length was exposed and clamped at both ends. NIH thrombin (500–1000 units) was introduced into the isolated vein segment, which was then gently kneaded for about 30 sec. Thrombi were allowed to form for approximately 20 min and then were released to the lungs.

Nine additional dogs were used in two control experiments. First, baseline ^{99m}Tc-DTPA clearance measurements were done as indicated below. In six of the animals, the subsequent experimental maneuver was confined to the transvascular insertion of an 8-Fr catheter that was atraumatically positioned either in the proximal (n = 3) or peripheral (n = 3) pulmonary vasculature. In three other animals, a catheter was positioned more centrally in the main pulmonary artery and Renografin-76 (25 cc) was injected at a rate of approximately 10 cc/sec to simulate the catheter positioning contrast dose. These experiments were done to determine if either catheter placement or doses of Renografin alone had significant effects on radioaerosol clearance.

Peripheral pulmonary vascular pressure was assessed in three additional animals. In these animals, the cobra catheter was replaced with a 7-Fr Berenstein 13-mm occlusion balloon catheter and a second cobra-style catheter was introduced through the opposite groin and positioned just proximal to the occlusion balloon. The occlusion balloon was positioned at approximately the segmental level. Once both catheters were positioned, the balloon of the occlusion catheter was inflated with dilute radiographic contrast to effectively occlude the distal lower lobe pulmonary artery. The exact position of the catheter and adequacy of the arterial occlusion was confirmed by an injection of Renografin through the proximally placed cobra catheter. Arterial pressure measurements were then obtained in the pulmonary artery segment just proximal and just distal to the occlusion balloon with the balloon inflated and deflated. Pulmonary arterial pressures were monitored by a Hewlett-Packard (Palo Alto, CA) physiologic monitor.

Scintigraphic Studies

Each animal underwent a baseline radioaerosol inhalation study in which ^{99m}Tc-DTPA radioaerosol (x = 37 MBq pulmonary deposition) was inhaled from a commercially available aerosol unit that generates submicronic polydisperse radioaerosol particles. The animals were positioned supine in a holding device under a Picker 4/11 gamma camera (Bedford, OH) interfaced to a data storage and analysis computer system (Macintosh-PC). Inhalation continued until the count rate reached 100,000 counts per second. At this point, the radioaerosol unit was disconnected from the animal's endotracheal tube and a quantitative clearance study began. Sequential 64 × 64 frames were collected at 15-sec intervals for 30 min. At the end of this time, a series of six 100,000-count digital 128 × 128 radioaerosol images (anterior, posterior, both right and left anterior and posterior obliques) were acquired. Postvascular occlusion radioaerosol studies were identical and were followed by six-view perfusion studies as described below.

Immediately after embolization or vascular occlusion, each anesthetized dog was moved to the room next to the angiographic suite, where the gamma camera was located, for imaging and clearance studies. Each dog was placed immediately beneath the scintillation camera and the radioaerosol deposition and clearance images were acquired as described above. As soon as the radioaerosol study had been completed, the animal was injected with 185 MBq of ^{99m}Tc-MAA and 500,000-count static perfusion images were obtained in the same six views described for the radioaerosol study. The purpose of these perfusion images was to document the persistence of vascular occlusion in the expected region for all animals that had undergone balloon occlusion and to verify the location and size of perfusion defects that had been created by autologous thromboemboli. The perfusion images also served as a guide for region of interest (ROI) selection for subsequent quantitative analysis of radioaerosol clearance rates.

Data Analysis

Clearance rates were calculated using the method recommended by Coates (5,6). A least square single exponential fit was made to the first eight minutes of clearance data from the respective areas of interest. A Tc-99m DTPA aerosol clearance rate from the lung was calculated from which the clearance half-time was determined. As Coates (5,6) demonstrated, this approach provides accurate determinations of clearance rates at a time when relative changes in background counts are minimal and at which simultaneous background correction is not required.

Four types of ROIs were used in the quantitative radioaerosol clearance analysis: (1) a ROI was inscribed on the first aerosol clearance frame that matched the perfusion defect of interest in each of the balloon occlusion experiments and all clearly identifiable perfusion defects in each of the thromboembolization experiments. Such regions are referred to as the occlusion area or PE area; (2) a zone approximately 5 pixels wide and immediately adjacent to the occluded area was also inscribed to assess contiguous zone clearance. These areas typically were superior to the occlusion zone; (3) whole-lung ROIs were inscribed around the lung that contained the occluded or embolized zone and around the opposite lung; and (4) a central rectangular-shaped ROI was inscribed bilaterally in the perihilar region that covered approximately the central third of the lung. The counts deposited in this central region were compared to those deposited in a region that outlined the remainder of each lung at baseline and after vascular occlusion. This central-to-peripheral radioaerosol count ratio

(i.e., penetration index) was assessed to determine if vascular occlusion had caused a shift in radioaerosol deposition patterns that might account in part for changes in postocclusion clearance rates.

Image Analysis

Six-view radioaerosol deposition image sets were arranged in randomized, independent order without identification as balloon occlusion, embolization or control experiments, and were presented to an independent observer for analysis. Included were nine of the special control studies as well as each of the 16 baseline and experimental image sets. Thus, a total of 41 randomized sets were reviewed. The observer was presented with a diagram of the lungs and asked to draw on the diagram any aerosol defects or hot spots that were present. In addition, the observer was required to note his degree of confidence regarding the presence of abnormalities on a five-degree scale (4 = defect definitely present to 0 = no defect). Only abnormalities seen with high confidence (category 4 or 3) were considered to be present for scoring purposes. Subsequently, the images were recollated and pre-experimental controls were matched with postexperimental studies. Any defects that had been noted in the same location on both control and experimental studies of the same animal were considered to be pre-existent and were excluded from further analysis. All statistical analyses were performed using paired t-tests.

RESULTS

Control studies showed generally uniform and symmetric radioaerosol deposition. Chest radiographs revealed that no opacities or volume loss had been induced by the experimental procedures. New radioaerosol deposition defects were seen with confidence in two of seven dogs distal to the site of a peripheral vascular balloon occlusion (Fig. 1) and in one of five dogs that had autologous thromboemboli. This latter defect was the only radioaerosol defect seen in conjunction with a total of 20 perfusion defects in the five animals with PE. No radioaerosol deposition defects or deposition asymmetries were identified in the four animals with central balloon occlusions. Thus, a total of three definite deposition defects were induced in the 16 dogs. None of the animals showed induction of focal aerosol hyperdeposition.

Baseline whole-lung radioaerosol clearance rates averaged 28.7 ± 9.2 min in the various groups. Slight but statistically insignificant lengthening of radioaerosol clearance rates was seen in regions of lung distal to central balloon occlusions (n = 4) (Fig. 2). Clearance rates in lungs opposite a central occlusion were, however, substantially faster than baseline (mean control half-time = 27.0 ± 3.3 min versus 15.4 ± 4.0 min experimental, p < 0.05).

Radioaerosol clearance rates were significantly faster in areas distal to peripheral balloon occlusions (Fig. 3). Clearance half-time declined from baseline rates of 33.6 ± 4.6 min to 19.0 ± 8.3 min (p < 0.05). The average clearance rate in the area immediately adjacent to the occluded zone was even faster (mean half time = 15.7 ± 10.1). Clearance throughout the same lung in which the peripheral balloon occlusion occurred was at virtually the same rapid rate as in the area distal to the occlusion itself. In one animal in
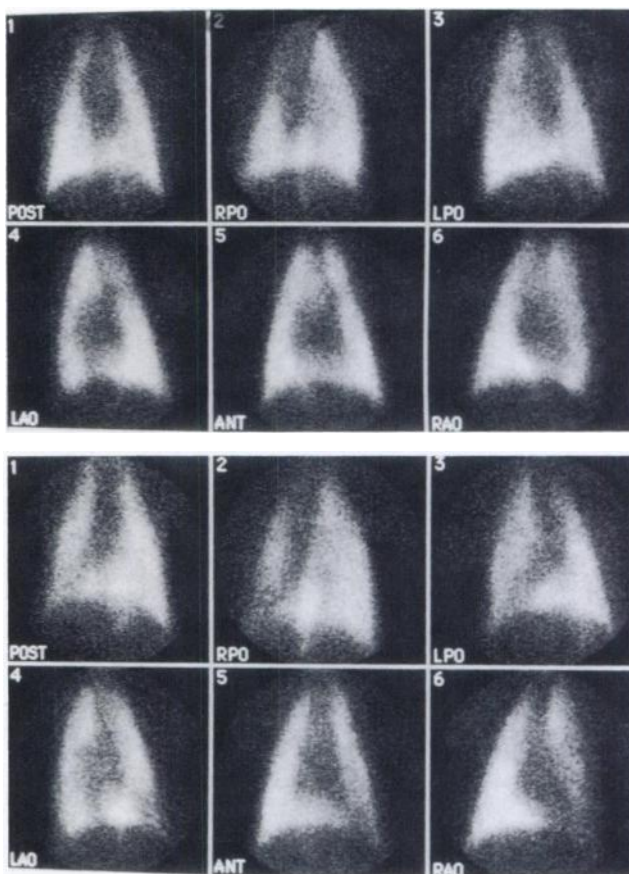

FIGURE 1. Baseline (A) and postvascular occlusion (B) ^{99m}Tc-DTPA radioaerosol images obtained 2 days later. In this animal, peripheral balloon occlusion was used. The balloon was inflated in a fourth-order vessel in the left lower lobe. The postocclusion images (B) show a new aerosol defect in the left lower lobe. The defect can be seen in every view, but is most obvious in the left lung base in the RPO and RAO views, as well as in the LAO and LPO views.

this group the balloon vascular occlusion caused such a marked unilateral change in clearance rates that the instrumented lung appeared asymmetrically hypoactive in the static radioaerosol images (Fig. 4). This was the only instance of this type seen in this study. There was no significant effect on clearance rates in the contralateral lung in any animal undergoing a unilateral peripheral vascular balloon occlusion.

The results in animals undergoing thromboembolism were even more dramatic than those created by the peripheral balloon model. The average clearance half-time in the five animals during the baseline study again was approximately 30 min. In 20 surveyed regions distal to thromboemboli, the clearance rate was more than twice as fast (mean half-time = 12.4 ± 3.7 min, p < 0.01). Once again, areas immediately adjacent to the embolized zone showed similar enhancement of radioaerosol clearance rates (Fig. 5). Based on the multifocal character of the thromboemboli, it was not possible to assess control regions in the same lung or contralateral lung.

The insertion of nonocclusive catheters into the proximal or peripheral pulmonary vasculature in six animals had
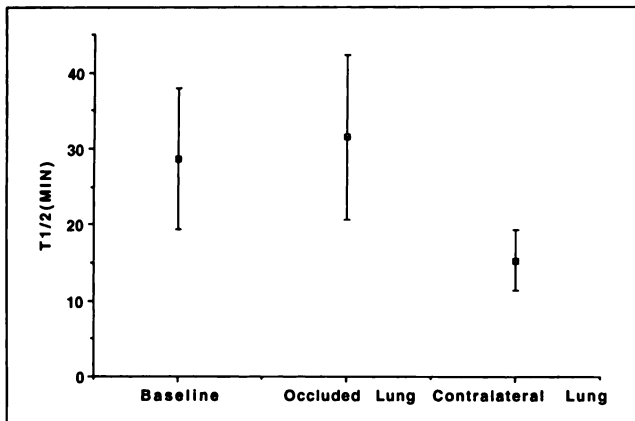
FIGURE 2. Radioaerosol clearance half-times (±1 s.d.) in the central balloon vascular occlusion group (n = 4 each data point). The slightly slowed clearance in the occluded lung is expected secondary to diminished blood flow. Accelerated clearance in the contralateral lung is statistically significant (p < 0.05).

no significant effect on radioaerosol clearance. The average clearance half-time declined from 28.0 ± 4.1 min (baseline) to 27.5 ± 6.5 min in the same lung in which the nonocclusive catheter was placed. Contralateral lungs showed no change in the clearance rate. Similarly, injection of contrast media alone (n = 3) had no significant effect on radioaerosol clearance. The mean aerosol penetration index was virtually the same in controls (1.02, n = 28) and after vascular occlusion (ratio = 0.99). Thus, there was no evidence of a radioaerosol deposition shift after vascular occlusion.

In experiments designed to evaluate if pulmonary arterial pressure changes were being created by peripheral balloon occlusion, there were no significant changes proximal to the inflated balloons. Average pulmonary arterial pressures rose from 22.7 ± 8.3 mm Hg to 24.0 ± 9.6 mmHg (n = 3). Thus, we could not implicate significant pressure changes with secondary vascular recruitment as the primary cause of increased radioaerosol clearance in the peripheral vascular occlusion model.

DISCUSSION

The results of the current studies suggest that both the deposition and clearance rates of ^{99m}Tc-DTPA radioaerosols are altered in the interval immediately following acute thromboembolism or catheter occlusion of the pulmonary vasculature. Localized defects in radioaerosol deposition that might alter interpretation of scintigraphic ventilation-perfusion studies of PE occurred relatively infrequently, but significant changes in clearance rates occurred consistently. Significantly different radioaerosol clearance changes were induced by central versus peripheral balloon occlusion. This suggests that a combination of mechanical and humoral factors are involved in creating the observed findings (see below). Emboli-induced changes were similar to those induced by peripheral balloon occlusion, but were more profound and more consistent. Because of this

study's ultimate attention to models that most closely simulate PE, peripheral balloon occlusion and autologous emboli became the foci of the investigation.

Occasional induction of focal radioaerosol deposition defects by peripheral balloon vascular occlusion or PE is not surprising. The frequency with which visible defects were induced in the current study is similar to that seen in previous studies using animal models to investigate emboli-induced abnormalities in the distribution of radioactive gases such as ^{133}Xe (2,3). It is worth noting that in the current study the radioaerosols were delivered to animals under nearly optimum conditions for peripheral penetration, i.e., propelled by a volume-cycled ventilator through an endotracheal tube. In clinical settings where patients with chest pain or chronic lung diseases inhale radioaerosols less effectively, the rate at which radioaerosol defects are induced by acute vascular occlusion might be higher than reported in the current study.

The early work of Isawa and Taplin (2) suggested that induced ventilation abnormalities occur in the immediate postembolic period and are transient. The current study was not designed to evaluate the temporal course of these events with respect to radioaerosols, but until proven otherwise one would suspect that PE-induced radioaerosol deposition defects would be similarly transient. In the clinical setting of PE, the temporal relationship between a scintigraphic examination and the actual occurrence of emboli is virtually impossible to determine. Thus, in general, the current findings do not contradict previous work that has established the utility of radioaerosol imaging in the assessment of the match/mismatch of ventilation and perfusion in patients with suspected PE.

The cause of the rare focal radioaerosol deposition defects seen in the current study is not clear. Previous studies (7) involving radioaerosol inhalation in dogs that had unilateral pulmonary fibrosis induced by hemithorax irradia-
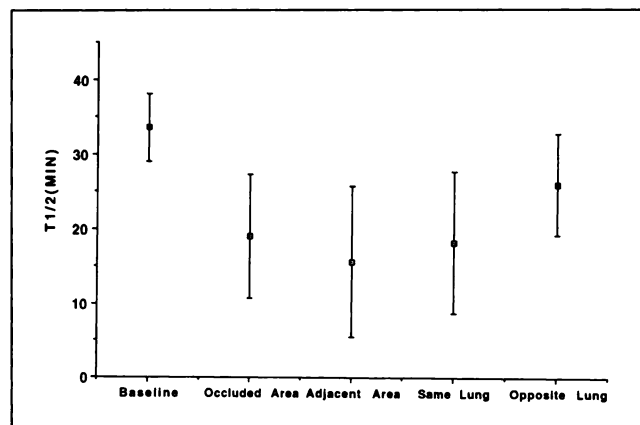
FIGURE 3. Radioaerosol clearance half-times (±1 s.d.) in the peripheral vascular occlusion group (n = 7 each data point) at baseline and in the immediate postocclusive period. Regions of interest defined in text. The clearance rates in the occluded zone, adjacent zone and ipsilateral lung all were significantly (p < 0.05) faster than baseline.
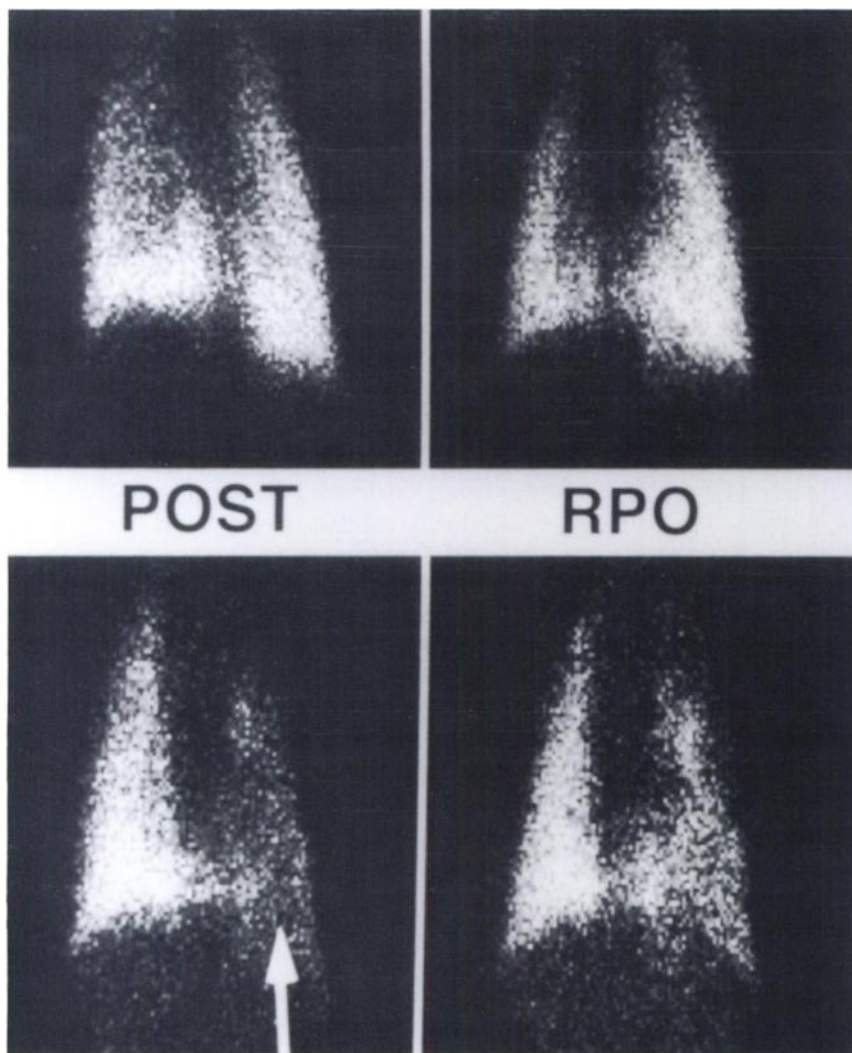
FIGURE 4. Selected baseline radioaerosol images (top) and postprocedure images (bottom) obtained 30–45 min after balloon occlusion of a fourth-order right lower lobe pulmonary artery in the same animal. Postocclusion, the right lung (arrow) appears to contain fewer radioaerosol counts than the left. Early postocclusion radioaerosol frames (not shown) appeared symmetric. The baseline right lung ^{99m}Tc-DTPA clearance half-time (31.1 min) shortened dramatically to 13.2 min after balloon vascular occlusion, while the left lung clearance half-time actually became slightly longer ($T_{1/2}$ baseline = 29.1 versus 30.9 min after instrumentation of the opposite lung). No other animal undergoing balloon vascular occlusion or having autologous PE demonstrated visible clearance-phase asymmetries or such substantial clearance rate changes.

tion have shown that radioaerosols do not enter noncompliant lung zones. Numerous investigators have reported that "stiffening" of the lung occurs transiently after acute embolization. If this phenomenon is enhanced in the region immediately beyond the embolus, radioaerosols could be preferentially diverted to other nearby lung zones, thus creating a local deposition defect. Rapid clearance of radioaerosol distal to the occlusion probably was not the dominant factor producing the defects seen in the current study. Radioaerosol clearance rates adjacent to and remote from the vascular occlusion in the same lung in our study were also accelerated. This would diminish the chances of seeing a localized defect, at least in the immediate postembolic period.

The previous work of Buxton-Thomas, et al. (4) showed accelerated DTPA clearance in embolic zones, but not in the "normal" portion of the same lung. The current results differ in that regard. In the current study, radioaerosol clearance rates were accelerated to the same degree in zones immediately adjacent to the embolized or occluded area and were significantly accelerated even in more remote regions of the same lung. Differences between the

Buxton-Thomas results and those of the current study may be explained by the different temporal relationships that existed. The patients in the Buxton-Thomas study had radioaerosol clearance rates determined by an independent radioaerosol inhalation study performed 24 hr after their original radioaerosol-perfusion study had suggested the high likelihood of PE. The temporal relationship of the first aerosol-perfusion study to actual embolization was, of course, unknown. Thus, it is certain that the Buxton-Thomas patients were at least 24 hr postembolization when their radioaerosol clearance rates were studied, and it is likely that many or most were even further removed from the embolic event. In the current study, however, changes in radioaerosol clearance rates were assessed in the immediate postocclusion or postembolism interval. Further studies will be required to evaluate the temporal resolution of these phenomena.

The current investigation was not designed to determine the etiology of increased ^{99m}Tc-DTPA clearance following vascular occlusion, but several preliminary observations seem relevant. The phenomenon of catheter-induced changes in radioaerosol clearance does not appear to be
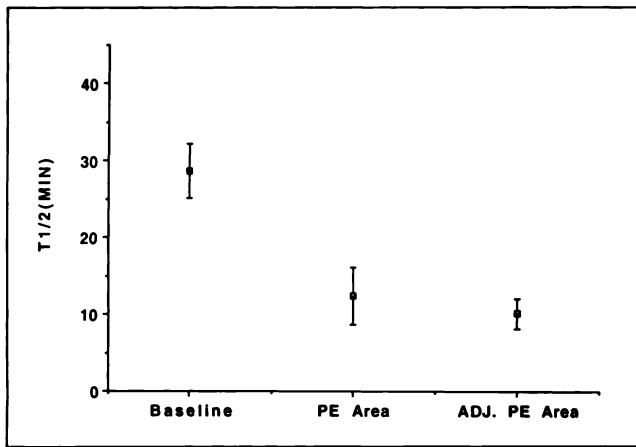
FIGURE 5. Radioaerosol clearance half-times (±1 s.d.) in the autologous thromboemboli group (n = 7 each data point). Both the zone distal to embolization and the adjacent zone cleared much (p < 0.01) faster than at baseline.

pressure-mediated recruitment of pulmonary vessels. Our evaluation showed that no significant increases in pulmonary vascular pressure were induced by peripheral vascular occlusion. Accelerated radioaerosol clearance was more likely mediated by humoral factors or vagal tone. The presence of catheters and balloons in contact with the pulmonary endothelium could cause elaboration of humoral factors such as prostacyclin, which could dilate remote pulmonary vessels or affect the alveolar-capillary membrane directly.

Increased vagal tone could cause regional bronchoconstriction with secondary distal air trapping and inflation of alveoli. This would provide larger alveolar surface areas for aerosol absorption through portions of the lung that are well perfused. Bronchoconstriction could also cause shifts in radioaerosol deposition. Technetium-99m-DTPA is absorbed from both alveolar and bronchial sites (8,9), but alveolar absorption is much more rapid (9,10). Thus, a peripheral shift of radioaerosol into zones dominated by alveoli might enhance clearance. Such deposition shifts were not seen in the current study, however. Another possibility is that acute vascular occlusion resulted in an immediate enhancement of bronchial blood flow, which in turn enhanced radioaerosol clearance. Such increases in bronchial blood flow are known to occur (11), but could not be assessed as part of the current study. Further studies to evaluate the potentially complex etiology of accelerated radioaerosol clearance secondary to vascular occlusion are now underway.

The increases in radioaerosol clearance associated with balloon occlusion of the pulmonary vasculature were unanticipated and may have clinical implications beyond the scope of lung scintigraphy. Radioaerosol clearance rates have been proposed as a means to monitor alveolar-capillary membrane integrity in the adult respiratory distress syndrome, lung transplant rejection and other pulmonary disorders (12–16). Patients with such disorders are fre-

quently in intensive care units. During the course of sequential DTPA radioaerosol clearance evaluations such patients may have Swan-Ganz wedge catheters or other instruments wedged into their pulmonary vasculature. Based on the findings of the current study, one might speculate that such vascular perturbation would cause at least transient changes in radioaerosol clearance rates. Such changes, depending on their temporal stability, might further confound the already complex group of variables impacting the reliability of DTPA measurements for monitoring patient course or response to therapy. Conversely, the degree and stability of such an alveolar response to vascular perturbation could, if standardized, conceivably be developed as a test of endothelial responsiveness.

Soluble radioaerosols of ^{99m}Tc-DTPA are the most completely studied and widely used among the radioaerosols employed as adjuncts to perfusion scintigraphy in the diagnosis of PE. The current findings suggest caution in interpretation of matched perfusion defects in aerosol-perfusion scintigrams when clinical events indicate that the emboli might have occurred in the immediate past. The current results also emphasize the dynamic nature and complexity of the factors impacting on the deposition pattern and transalveolar clearance of these radioaerosols. Further studies of these factors seem warranted to enhance our understanding of the potentials of radioaerosols for studying pulmonary disorders associated with pathologic or iatrogenic perturbations of the pulmonary vasculature.

ACKNOWLEDGMENTS

REFERENCES

1. Austin JHM, Sagel SS. Alterations of airway caliber after pulmonary embolization in the dog. *Invest Radiol* 1972;7:135–139.
2. Isawa T, Taplin GV, Beazell J, Criley MJ. Experimental unilateral pulmonary artery occlusion—acute and chronic effects on relative inhalation and perfusion. *Radiology* 1972;102:101–109.
3. Alderson PO, Doppman JL, Diamond SS, Mendenhall KG. Ventilation-perfusion lung imaging and selective pulmonary angiography in dogs with experimental pulmonary embolism. *J Nucl Med* 1978;19:164–171.
4. Buxton-Thomas M, Higenbottam T, Barber R, Wraight P. Clearance of inhaled ^{99m}Tc-DTPA from regions of the lung recently affected by pulmonary embolus. *Bull Eur Physiopathol Respir* 1986;22:55–60.
5. Coates G, O'Brodovich H. Extrapulmonary radioactivity in lung permeability measurements. *J Nucl Med* 1987;28:903–906.
6. O'Brodovich H, Coates G. Pulmonary clearance of ^{99m}Tc-DTPA: a noninvasive assessment of pulmonary epithelial integrity. *Lung* 1987;165:1–16.
7. Alderson PO, Bradley EW, Mendenhall KG, et al. Radionuclide evaluation of pulmonary function following hemithorax irradiation of normal dogs with ^{60}Co or fast neutrons. *Radiology* 1979;130:425–433.
8. Oberdorster G, Utell MJ, Morrow PE, Hyde RW, Weber DA. Bronchial and alveolar absorption of inhaled ^{99m}Tc-DTPA. *Am Rev Respir Dis* 1986;134:944–950.
9. Bennett WD, Ilowite JS. Dual pathway clearance of ^{99m}Tc-DTPA from the bronchial mucosa. *Am Rev Respir Dis* 1989;139:1132–1138.
10. Ilowite JS, Bennet WD, Sheetz MS, Groth ML, Nierman DM. Permeability of bronchial mucosa to ^{99m}Tc-DTPA in asthma. *Am Rev Respir Dis* 1989;139:1139–1143.
11. Jindal SK, Lakshminarayan S, Kirk W, Butler J. Acute increase in anasto-

motic blood flow after pulmonary arterial obstruction. *J Appl Physiol* 1984; 57:424–428.

12. Jacobs MP, Baughman RP, Hughes J, Fernandez Vlloa M. Radioaerosol lung clearance in patients with active pulmonary sarcoidosis. *Am Rev Respir Dis* 1985;131:687–689.
13. Jeffries AL, Coates G, O'Brodovich H. Pulmonary epithelial permeability in hyaline membrane disease. *N Engl J Med* 1984;311:1075–1080.
14. Braude S, Nolop KB, Hughes JMP, Barucs PJ, Royston D. Comparison of lung vascular and epithelial permeability indexes in the adult respiratory distress syndrome. *Am Rev Respir Dis* 1986;133:1002–1005.
15. Herve PA, Silbert D, Mensch J, et al. Increased lung clearance of ^{99m}Tc-DTPA in allograft lung rejection. *Am Rev Respir Dis* 1991;144:1333–1336.
16. Rosso J, Guillon JM, Parrot A, et al. Technetium-99m-DTPA aerosol and gallium-67 scanning in pulmonary complications of human immunodeficiency virus infection. *J Nucl Med* 1992;33:81–87.